Nonlinear Free Energy Relationship in the General-Acid-Catalyzed Acylation of Rat Kidney γ-Glutamyl Transpeptidase by a Series of γ-Glutamyl Anilide Substrate Analogues†

Annie Ménard, Roselyne Castonguay, Christian Lherbet, Caroline Rivard, Yoann Roupioz, and Jeffrey W. Keillor*

Département de chimie, Université de Montréal, C.P. 6128, Succursale centre-ville, Montréal, Québec, Canada H3C 3J7

Received June 14, 2001; Revised Manuscript Received August 8, 2001

ABSTRACT: The γ-glutamyl transpeptidase (GGT) purified from rat kidney reacts with a series of eight parasubstituted L-glutamyl γ-anilides, in the presence of Gly−Gly, catalyzing the formation of γ-Glu−Gly−Gly (pH 8.0, 37 °C). The transpeptidation reaction was followed through the discontinuous colorimetric determination of the concentration of released parasubstituted aniline. Steady-state kinetic studies were performed to measure k_{cat} and K_M values for each anilide substrate. A Hammett plot constructed by the correlation of log(k_{cat}) and the σ^- parameter for each anilide substrate displays statistically significant upward curvature, consistent with a general-acid-catalyzed acylation mechanism in which the geometry of the transition state changes with the nature of the para substituent. Kinetic isotope effects were measured and are consistent with a reaction involving a proton in flight at the rate-limiting transition state. The pH-rate profiles measured over pH 7.0−9.5 are bell-shaped with kinetic pK_a values that may be attributed to the active site nucleophile (or its general-base catalytic partner) and the active-site general acid. The variation of the latter pK_a value as a function of temperature is consistent with an enthalpy of ionization expected for an ammonium ion acting as a general acid. Examination of the variation of k_{cat} as a function of temperature gave values for the enthalpy and entropy of activation that are similar to those determined for the general-acid-catalyzed breakdown of the tetrahedral intermediate formed during acylation of chymotrypsin by similar amide substrates.

γ-Glutamyl transpeptidases (GGT, EC 2.3.2.2) are highly glycosylated enzymes bound to the extracellular membrane of cells that play roles in secretion and absorption processes, such as epithelial and lymphoid cells. GGT plays important physiological roles in the degradation and synthesis of glutathione (GSH) and the γ-glutamyl cycle (*1*−*3*), which allows the transport of some amino acids across the cellular membrane (*4*). Furthermore, GGT is implicated in the cellular detoxification process through its catalysis of the hydrolysis of thioconjugates formed between glutathione and drugs or metabolic waste products, generating mercapturic acids which are easily eliminated in urine (*3*).

The principal chemical reaction catalyzed by GGT is the acyl transfer of the γ-glutamyl group of GSH, *S*-conjugates of GSH, and other γ-glutamyl derivatives (*5*−*8*), including L-γ-glutamyl-*p*-nitroanilide, an excellent substrate for this enzyme (*7*−*9*). GGT is known to transfer this γ-glutamyl group to a large variety of acceptors. When the acceptor substrate is an α-amino acid or a dipeptide, the transfer reaction is referred to as a transpeptidation reaction, of which a commonly studied example is the reaction occurring between L-γ-glutamyl-*p*-nitroanilide as an acyl donor and Gly−Gly as an acyl acceptor to give γ-glutamylglycylglycine, γ-Glu−Gly−Gly (*10*).

L-γ-Glutamyl derivatives, which serve as good donor substrates, may also react as acceptor substrates in an autotranspeptidation reaction when present in high concentrations (*11*). However, this reaction can be avoided by using concentrations of donor substrate which are much lower than the value of their apparent K_M as acceptors, or by using D-γ-glutamyl derivatives, which act as acyl donors, but cannot act as acceptors (*11*, *12*). Water can also act as an acceptor, resulting in the hydrolysis of the γ-glutamyl bond to give glutamic acid (*11*−*13*). Some investigators have suggested that GGT serves primarily to hydrolyze γ-glutamyl derivatives rather than catalyze their amine transfer reactions under physiological conditions (*14*).

Although GGT has been studied for a number of years by many research groups and is of broad physiological importance, its mode of action is not very well understood. The most probable mechanistic model for GGT catalysis suggested in the literature is a modified "ping-pong" mechanism (*11*−*12*), where acylation of the free enzyme is followed by a deacylation step, via either hydrolysis or aminolysis (Scheme 1), although some investigators have suggested that

† This research was supported by Operating Grant # OGP0184034 from the Natural Sciences and Engineering Research Council (NSERC) of Canada. In addition, R.C. and C.L. gratefully acknowledge the financial bursary support of NSERC and the Université de Montréal, respectively.

* To whom all correspondence should be addressed. Tel.: (514) 343-6219. Fax: (514) 343-7586. E-mail: keillorj@chimie.umontreal.ca.

[1] Abbreviations: CHES, 2-[*N*-cyclohexylamino]ethane sulfonic acid; DON, 6-diazo-5-oxo-L-norleucine; GGT, γ-glutamyl transpeptidase (EC 2.3.2.2); GSH, glutathione (γ-Glu−Cys-Gly); kie, kinetic isotope effect; MOPS, 3-[*N*-morpholino]propane sulfonic acid; Tris, tris(hydroxymethyl)aminomethane.

10.1021/bi011234d CCC: $20.00
Published on Web 09/27/2001

Scheme 1

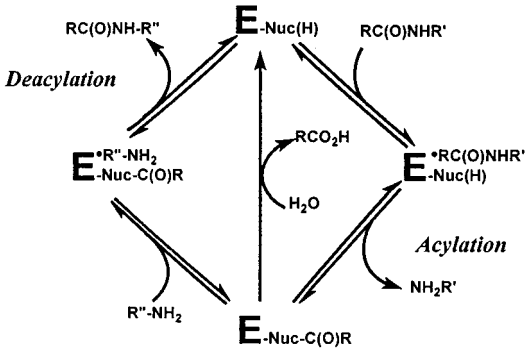

the mechanistic pathway is sequential, with random addition of substrates and ordered release of products (*15*). Currently, the amino acid residues involved in the enzymatic catalysis of rat kidney GGT, including the active site nucleophile, have not been identified. A deeper comprehension of the catalytic mechanism of mammalian GGT is clearly critical to the future development of efficient drugs for the treatment of certain cellular disorders as well as to counteract the effect of GGT in the resistance against certain medications. In the past, the mechanism has been studied extensively using γ-glutamyl *p*-nitroanilide, a compound known to be a good substrate for the enzyme (*8*, *11*, *12*, *16*) which liberates highly colored *p*-nitroaniline upon its reaction with GGT. In the present study, we describe the preparation of a series of parasubstituted γ-glutamyl anilide substrate analogues and their use in detailed kinetic studies of the mechanism of the acyl transfer reactions catalyzed by GGT purified from rat kidney. These studies include an investigation of the substituent effects, kinetic isotope effects, and the effects of pH and temperature on the enzyme-catalyzed reaction.

MATERIALS AND METHODS

Materials. BioGel A-0,5m (50−100 mesh) and Bradford protein assay solution were purchased from Bio-Rad. BSA (bovine serum albumin, Fraction V) and papain (14 U/mg) were purchased from Sigma-Aldrich. All aqueous solutions were prepared from water deionized and purified by a Millipore Milli-Q BioCell system.

Protein concentration was determined by the Bradford assay (*17*). The specific activity was determined according to a previously described method (*8*, *9*) using final concentrations of 1 mM γ-glutamyl-*p*-nitroanilide and 20 mM Gly−Gly in Tris−HCl buffer (pH 8.0) and an extinction coefficient of released aniline of 8800 M^{-1} cm^{-1}. One unit of activity is defined as the release of one micromole of *p*-nitroaniline in one minute at 37 °C. All absorbance measurements were made using either a Milton-Roy Spectronic 1201 or a Varian Cary 100 spectrophotometer.

The substrate analogue anilides shown in Figure 1 were synthesized according to the detailed procedure provided in the Supporting Information.

Enzyme Purification. Kidneys of adult male Sprague−Dawley rats were either purchased from Rockland, Inc. (Gilbertsville, PA), or obtained as a generous gift from either Dr. C. Desrosiers of Notre Dame Hospital (Montréal, QC) or Dr. S. Rowland of Merck-Frosst (Pointe-Claire, QC). The kidneys were prepared essentially according to the procedure of Malathi et al. (*18*), except that the kidneys were not

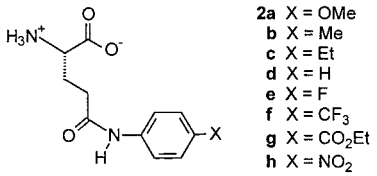

FIGURE 1: Substrate analogues synthesized for the acylation of GGT in this study.

perfused prior to treatment. The GGT enzyme was isolated and purified from 17 g of kidneys according to the protocol of Tate and Meister (*8*, *9*), which was slightly modified as follows: The rat kidneys were frozen and dissected by scalpel to separate the cortex from the medulla and connective tissues. The cortexes were then homogenized using a Polytron 3000 homogenizer operated at 15000 rpm for 30 s. After the papain digest step, ammonium sulfate was added to the enzyme solution to 60% of saturation. After centrifugation (18000 × g, 30 min) of this solution, more ammonium sulfate was added to the supernatant fraction to 90% of saturation. The pellet resulting from centrifugation of this solution (18000 × g, 30 min) was resuspended and purified by size exclusion chromatography, using a 62 cm × 2.5 cm column of Bio-Gel A-0.5m (50−100 mesh) controlled by a Bio-Rad Econo-System. A volume of 350 mL of 0.05 M Tris-HCl buffer (pH 8.0) was used to elute the protein solution at 0.35 mL/min, giving 88 fractions of 4 mL. A volume of 26.5 mL of active enzyme (837 U/mg, 26 μg/mL) was collected and frozen at −20 °C. No significant loss of activity was detected over a period of 18 months at this temperature. Furthermore, once thawed and stored at 4 °C, the enzyme was stable for up to 3 months.

Methods. Colorimetric Determination of Aniline Concentration. The colorimetric determination of aniline through diazotization was based on the protocol of Goldbarg et al (*19*) and is described in detail in the Supporting Information. All standard curves were determined in duplicate for aniline concentrations ranging from 1 to 40 μM.

Steady-State Kinetics. Before each kinetic experiment, a standard specific activity assay was performed on the GGT to be used in order to confirm that its specific activity did not vary. All kinetic tests were carried out at 37 °C. The progress of the reaction of the γ-glutamyl anilide substrates was followed by the steady-state release of aniline according to the diazotization method described in the Supporting Information. A test tube was charged with 25−500 μL of a 5 mM stock solution of a given parasubstituted L-γ-glutamylanilide (pH 8.0) and 1500 μL of 0.1 M Tris-HCl buffer (pH 8.0). To this was then added 500 μL of 0.1 M glycylglycine (pH 8.0), and the volume was brought to 2.5 mL with the addition of 0−475 μL of 0.1 M Tris−HCl buffer (pH 8.0). For higher concentrations of anilide substrates, the anilide was added as a solid to the reaction mixture and completely dissolved by vortex. The reaction mixtures were incubated at 37 °C for 10 minutes, and the enzymatic reactions were initiated with the addition of 5−20 μL of a 100-fold dilution of the final purified enzyme solution. A 375 μL aliquot of the reaction mixture was taken every 5−10 min over a period of 80 min and added to 125 μL of 40% TCA. The diazotization of released aniline was then initiated according to the protocol described in the Supporting Information. Plots of the absorbance of the diazotized

Table 1: Kinetic Parameters (k_{cat}, K_M, and $\log(k_{cat}^X/k_{cat}^H)$) Obtained According to Equation 4 for the Reaction of GGT, in the Presence of 20 mM Gly−Gly at 37 °C at pH 8.0 (0.1 M Tris−HCl), with Substrates **2a**−**h** and Their Respective σ^- Values

substrate	k_{cat}[a] (s^{-1})	K_M[a] (μM)	$\log(k_{cat}^X/k_{cat}^H)$[b]	σ^-[c]
L-Glu(γ-*p*-methoxyanilide)	971	953	0.335	−0.27
L-Glu(γ-*p*-methylanilide)	834	594	0.269	−0.17
L-Glu(γ-*p*-ethylanilide)	544	647	0.083	−0.15
L-Glu(γ-anilide)	449	450	0.000	0.00
L-Glu(γ-*p*-fluoroanilide)	429	890	−0.020	0.15
L-Glu(γ-*p*-trifluoromethylanilide)	868	779	0.286	0.65
L-Glu(γ-*p*-ethoxycarbonylanilide)	834	1055	0.269	0.74
L-Glu(γ-*p*-nitroanilide)	1152	468	0.408	1.27

[a] Experimental error is estimated at ± 10%. [b] Experimental error is estimated at ± 0.046. [c] Hammett substituent parameters were taken from ref 22.

derivatives of the released aniline, as a function of time (representing less than 10% of the total reaction), were prepared for six concentrations, ranging from 50 to 2000 μM, of each anilide substrate. For each substrate concentration, a blank reaction was run by replacing the enzyme solution with the appropriate buffer. In all cases, these plots of absorbance versus time for each substrate concentration were found to be linear, with no evidence of a "burst" or "lag" in the absorbance. The slopes from these plots were transformed into initial reaction rates by dividing by the appropriate apparent extinction coefficients previously determined (ϵ^{app} in Table 1S in Supporting Information). These reaction rates were in turn corrected for the concentration and specific activity of the enzyme used (expressed in units of μM min^{-1} mg^{-1}). The observed reaction rates (v) showed a hyperbolic dependence on substrate concentration; nonlinear regression of the data according to eq 1 (using the curve-fitting software Axum 5.0) provided values for the kinetic parameters k_{cat} and K_M:

$$\frac{v}{[E]_0} = \frac{k_{cat}[sub]}{K_M + [sub]} \quad (1)$$

Isotope Effect Studies. To measure the isotope effect of the apparent transpeptidation reaction rate, the same procedure was used as reported above for kinetic studies, except that all solutions used in the reaction mixtures were prepared with D_2O. Reaction rates were followed over 40 min for seven concentrations of L-Glu(γ-*p*-nitroanilide), L-Glu(γ-anilide), and L-Glu(γ-*p*-methoxyanilide) ranging from 25 to 2000 μM. The pD values of the deuterated solutions were calculated by adding 0.4 to the values reported by the Fisher Accumet 15 pH meter equipped with a glass electrode (*20*).

pH−Rate Profile Experiments. The pH−rate profiles of the reactions of L-γ-glutamyl-*p*-methoxyanilide, L-γ-glutamyl-*p*-anilide, and L-γ-glutamyl-*p*-nitroanilide with purified GGT were constructed according to the same kinetic protocol described above, using 0.1 M buffer solutions to maintain reaction mixture pH values of 7.0 (MOPS), 7.5, 8.0, 8.5 (Tris-HCl), and 9.0 and 9.5 (CHES). At each pH, the glycylglycine stock solution was adjusted to the appropriate pH with the addition of either 2 N HCl or 2 M NaOH prior to addition to the reaction mixtures. The stability of GGT at the various pH levels studied was confirmed by incubating the enzyme in the various buffers for 40 min, followed by verification of its consistent specific activity according to a standard activity assay at pH 8.0. The observed k_{cat} values were found to vary as a function of pH according to eq 2, from which the macroscopic pK_a values pK_1 and pK_2 were determined:

$$k_{cat}^{obs} = \frac{k_{cat}}{\frac{[H^+]}{K_1} + 1 + \frac{K_2}{[H^+]}} \quad (2)$$

Temperature Effect Studies. The effect of temperature on k_{cat} for the reaction of GGT with L-γ-glutamyl-*p*-methoxyanilide, L-γ-glutamyl-*p*-anilide, and L-γ-glutamyl-*p*-nitroanilide was studied essentially according to the same kinetic protocols described above, at temperatures between 15 and 50 °C. The reaction solutions were incubated at the desired temperature for 10 min prior to initiating the reactions with the addition of enzyme.

RESULTS AND DISCUSSION

Synthesis and Steady-State Kinetics. Many kinetic studies of GGT have been carried out using L-γ-glutamyl-*p*-nitroanilide as an acyl donor substrate (*8*, *9*, *11*, *12*, *16*). In the present study, we have prepared the series of novel parasubstituted γ-glutamyl anilides shown in Figure 1 using a general procedure based on a previously published protocol (see Scheme 1S and Materials in Supporting Information). The reaction of GGT with this series of substrate analogues **2a**−**h** in the presence of glycylglycine as an acyl acceptor was followed using the discontinuous colorimetric aniline diazotization assay described in the Supporting Information. Steady-state kinetic parameters were obtained according to eq 1 (see Methods). In this way, our synthetic substrate analogues permitted an investigation of substituent effects on the catalyzed transpeptidation reaction.

Rate-Limiting Acylation Step. Control experiments were performed in order to establish that, under the reaction conditions employed, the observed reaction is the transpeptidation resulting from the transfer of a γ-glutamyl group from our series of L-γ-glutamyl anilides to glycylglycine used as an acceptor substrate. For example, at the relatively high concentration (20 mM) of Gly−Gly used, the transpeptidation reaction rate is independent of Gly−Gly concentration and is the predominant enzymatic reaction, since the background enzymatic hydrolysis and autotranspeptidation reactions possible with L-glutamyl donor substrates account for less than 2% of the observed activity (*8*, *9*, *11*, *12*, *16*, *21*). The use of a high concentration of Gly−Gly, an efficient acceptor substrate, also ensures that under the reaction conditions of this kinetic study, the deacylation step is fast, making the acylation step rate-limiting and kinetically pertinent.

Hammett Plot for Acylation Step. Shown in Table 1 are the kinetic parameters obtained for substrate γ-glutamyl anilides **2a**−**h**, along with the σ^- values (*22*) used to construct the plot shown in Figure 2. The obvious nonzero slope of this plot indicates that the rate constant for the enzymatic reaction varies according to the parent aniline, which is the leaving group for the acylation reaction, confirming that acylation is the rate-limiting step of the enzymatic reaction under these conditions. In sharp contrast to these results, the rates measured for the enzymatic

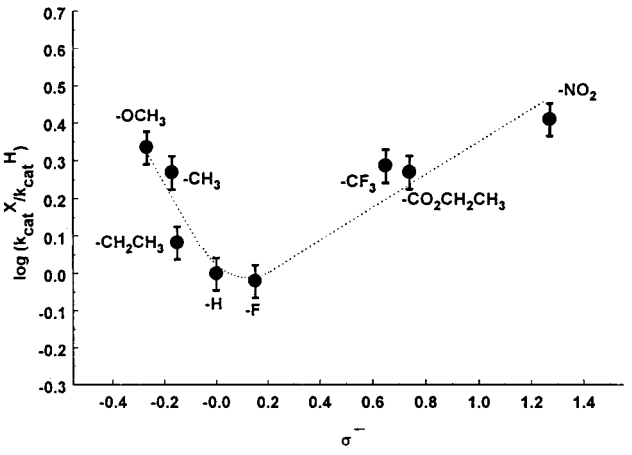

FIGURE 2: Hammett plot of the kinetic data obtained according to Equation 4 for the reaction of rat kidney GGT with a series of parasubstituted L-Glu(γ-anilide) substrates in the presence of 20 mM Gly−Gly, pH 8.0 (0.1 M Tris-HCl), 37 °C (see Table 1 and Methods). The dotted lines through the data are intended only to emphasize the significant upward curvature of the data and are the result of linear regression of the four leftmost data points ($\rho = -1.3 \pm 0.4$) and the four rightmost data points ($\rho = +0.4 \pm 0.1$).

hydrolysis reaction in the absence of acceptor substrate are much slower and show no dependence on the para substituent of the γ-glutamyl anilide substrate (*21*). Clearly, deacylation is rate-limiting in the case of hydrolysis but sufficiently rapid in the presence of a high concentration of a suitable acceptor substrate (i.e. 20 mM Gly−Gly) such that acylation becomes rate-limiting under these conditions.

Although both k_{cat} and k_{cat}/K_M values were plotted against a variety of parameters (not shown), including σ_I and σ_R, Taft steric parameters, and van der Waals volumes, only the combination shown in Figure 2 (i.e., k_{cat} vs σ^-) demonstrated any significant correlation. The correlation between the σ^- values and k_{cat} (but not σ^- and k_{cat}/K_M) suggests that the rate-limiting step of the acylation process involves the reaction of a covalent reactive intermediate along the reaction pathway (*22*), such as the breakdown of a tetrahedral intermediate formed upon the attack of the active site nucleophile on the carbonyl group of the substrate anilides, known to form tetrahedral intermediates in their acyl-transfer reactions (*23*). Apparently, the variation of K_M values within the series of parasubstituted anilides **2a**−**h** is due to a complex combination of electrostatic, dipolar, steric, or hydrophobic interactions of the para substituents themselves with the extended γ-glutamyl donor binding site, remote from the site of chemical reactivity, that contribute to the affinity of the substrates without systematically affecting their reactivity.

The most conspicuous feature of Figure 2 is the upward curvature of the correlation. The statistical significance of this upward curvature was confirmed by completely repeating the experiments, including the purification of the enzyme, the synthesis of the substrates, and the preparation of all solutions. Upon such a thorough repetition, the deviation of the values of k_{cat} was found to be within 10%, indicating that the plot was indeed biphasic, displaying a negative slope between the electron donating substituent substrates ($\rho = -1.3 \pm 0.4$) and a positive slope among the electron-withdrawing substituent substrates ($\rho = 0.4 \pm 0.1$). The upward curvature of Figure 2, observed for L-glutamyl-γ-anilides **2a**−**h**, was also observed with a series of D-glutamyl-γ-anilide substrates synthesized according to the route given in the Supporting Information starting from D-glutamic acid (*21*). Since D-glutamyl derivatives are known to function as acyl donors, but not acyl acceptors (*8*, *9*, *11*, *16*), they are incapable of participating in autotranspeptidation, further confirming that the observed phenomenon is a feature of the enzymatic transpeptidation reaction.

The observed upward deviation from linearity of the Hammett plot indicates there are apparently two ways to accelerate the enzymatic acylation reaction over that of γ-glutamylanilide (roughly located at the minimum) that involve either electron-donating substituents or electron-withdrawing substituents. Typically, the upward curvature of Hammett plots is generally explained by invoking either a change in mechanism or a substituent-induced change of geometry of the rate-limiting transition state (*24*). These two possibilities will be considered in turn.

The putative change in the acylation mechanism is represented in Scheme 2. Pathway 1 of Scheme 2 shows the rate-limiting protonation of a tetrahedral intermediate, formed by the rapid attack of an active site nucleophile upon the γ-glutamylanilide, prior to rapid breakdown. This pathway would presumably be favored by substrates bearing electron donating substituents, which render the aniline nitrogen more basic and accelerate protonation; however, a protonation step

Scheme 2

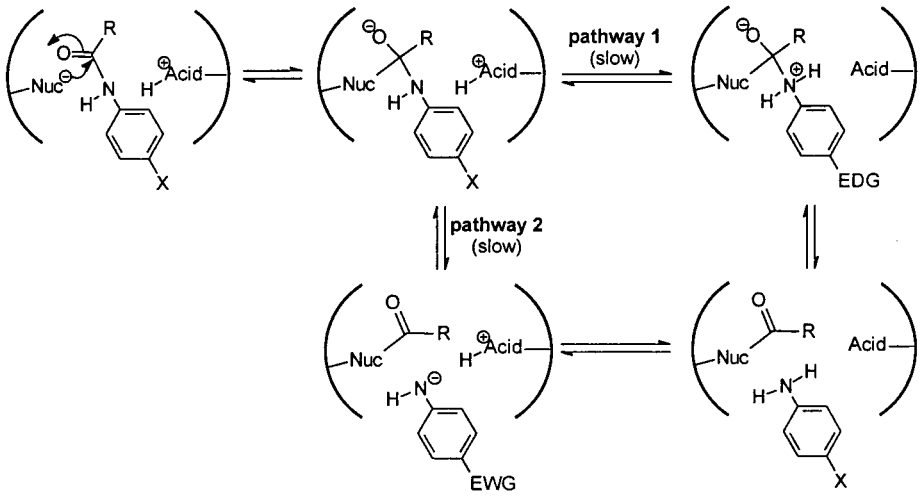

is unlikely to be rate-limiting in an enzymatic reaction, where an acidic group would be appropriately positioned to efficiently catalyze the reaction (*22*). In the case of substrates bearing electron withdrawing substituents, the mechanism shown in pathway 2 of Scheme 2 may be favored, wherein the rate-limiting departure of anilide anion would be accelerated by electron-withdrawing substituents and followed by rapid proton transfer to the anilide anion. The relatively high pK_a values of the corresponding anilines leads us to believe that this reaction pathway is improbable but not impossible, given the ability of enzymes to stabilize the formation of high energy anions (*25*, *26*.)

Conversely, the putative change in geometry of the rate-limiting transition state that would be consistent with the observed phenomenon may be explained by invoking a concerted general-acid-catalyzed acylation mechanism, as shown in Scheme 3. According to this pathway, the initially formed tetrahedral intermediate undergoes general-acid-catalyzed breakdown, wherein proton transfer to the nitrogen of the departing aniline occurs simultaneously with C−N bond cleavage. The degree of proton transfer and the C−N bond cleavage would both independently depend on the electronic nature of the para substituent. Electron withdrawing substituents would favor the cleavage of the amidic C−N bond, resulting in a transition state that features significant C−N bond lengthening. However, these same substituents would render the aniline nitrogen less basic, disfavoring its protonation, resulting in a transition state that features less proton transfer. In the case of electron-donating substituents, the effect would be reversed, giving a transition state characterized by less stretching of the C−N bond and more proton transfer from the active site general acid. The overall geometry of the transition state would therefore reflect the composite result of the competing effects of each para substituent, as shown in Figure 3 as a More-O'Ferrall−Jencks diagram. These appreciable differences in the geometries of the respective transition states represents a breach of the premise of linear free-energy relationships, which would manifest itself as an upward curvature of the corresponding log−log plot (*24*).

According to our proposed concerted mechanism, the charge developed on the nitrogen of the aniline leaving group would depend on the extent of protonation versus C−N bond cleavage realized at the transition state. By plotting the kinetic data of Figure 2 as a function of the pK_a of the conjugate acids of the leaving groups (i.e. the anilinium ions), the data could equally have been presented as a Brønsted plot. Since these pK_a values have been shown (*27*) to be related to the Hammett σ^- parameter (by the equation pK_a = 4.58−2.80 × σ^-), it is possible to determine the slopes (β_{lg}) that would be obtained for this re-plot. For the less basic anilines (bearing electron withdrawing substituents), $\beta_{lg} = -0.13 \pm 0.03$, whereas for the more basic anilines (bearing electron donating substituents), $\beta_{lg} = 0.46 \pm 0.15$. These values give an indication of the charge developed on the leaving group nitrogen at the transition state (*22*).

Linear (and nonlinear) free-energy relationships have long been used to characterize the transition states of many different types of reactions, some of which also display upward curvature (*28*−*32*). Typically, these reactions involve two competing mechanistic pathways that have opposing electronic demands or one concerted mechanism that features

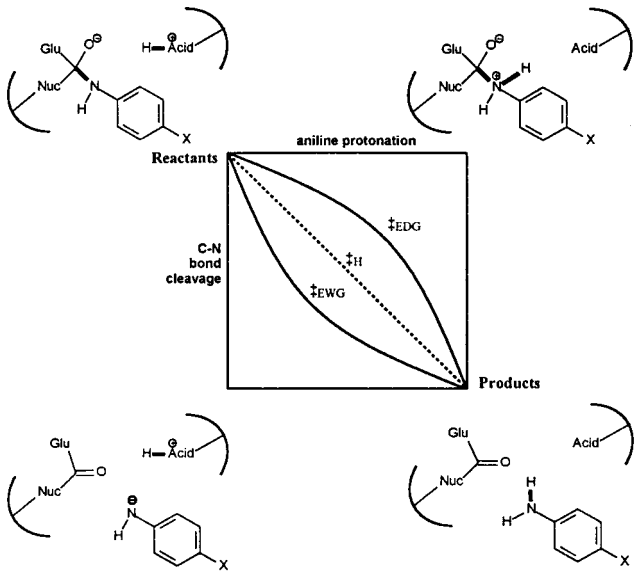

FIGURE 3: More O'Ferrall−Jencks diagram illustrating the effect of the leaving group substituent on the degree of leaving group protonation and C−N bond cleavage during rate-limiting acylation leading to the upward curvature of the Hammett plot shown in Figure 2.

Scheme 3

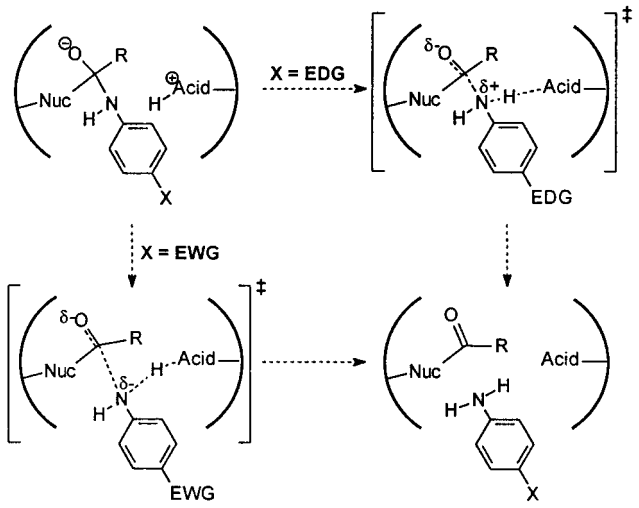

a transition state comprising two separate steps with opposing electronic requirements (*31*). It should be noted that generally the hydrolysis of amides in solution does not usually display such concerted behavior, since the sequential protonation and decomposition of a tetrahedral intermediate (Scheme 2, pathway 1) is not thermodynamically disfavored (*23*, *33*, *34*). However, in all cases, the stability of the protonated intermediate depends on its acidity relative to the kinetic general acid responsible for the leaving group protonation. Therefore, the relative basicity of the amine leaving group will determine whether the reaction is sequential or concerted. The zwitterionic tetrahedral intermediate of an anilide substrate would be relatively acidic, favoring a concerted reaction mechanism, and the substituent of the aniline leaving group would influence the geometry of the transition state of the concerted reaction.

Free-energy relationships have also been used to characterize the transition state of the rate-limiting step of enzymatic reactions (*35*), involving studies of substituent effects of

parent carboxylic acid derivatives (*36*, *37*) or leaving groups (*38*−*40*). Some studies have used amino acid anilide substrates similar to those used herein to study the acylation reactions of cysteine proteases (*41*) and serine proteases (*42*, *43*). For example, the rate-limiting acylation of the serine protease chymotrypsin by amino acid anilides has been extensively studied and is of particular relevance to our current work. Notably, it has been shown that the Hammett plot for this reaction curves upward (*44*−*47*), from a slope of ∼−2 with electron donating substituents (low σ) (*43*−*45*) to a slope of ∼0.7 for electron withdrawing substituents (high σ) (*44*,*47*). This curvature was explained in terms of the effect of the substituent on the degree of protonation of the aniline leaving group realized at the transition state (*44*). Our explanation of the upward curvature of Figure 2 is concordant with these similar lines of reasoning.

Isotope Effect Studies. Now, if in fact a change in mechanism were responsible for the observed curvature, then one would expect significantly different isotope effects for the two distinct mechanistic pathways shown in Scheme 2. In the case of acylation by substrates bearing electron donating substituents, the reaction is accelerated by facilitating rate-limiting protonation, which would be susceptible to a kinetic isotope effect (Scheme 2, pathway 1). However, in the case where acylation is accelerated by substrates bearing electron withdrawing substituents, the rate-limiting step must involve C−N bond cleavage, not proton transfer, and should not show a kinetic isotope effect (Scheme 2, pathway 2). On the other hand, if the observed upward curvature is due to a change in geometry of the rate-limiting transition state deriving from general-acid catalysis (Scheme 3), then acylation by substrates bearing either electron withdrawing or electron donating substituents would implicate transition states that involve proton transfer and may give rise to kinetic isotope effects. The following experiment was designed in order to distinguish between these two possibilities.

The values of k_{cat} were measured in D_2O for three representative substrates whose water k_{cat} values defined the curvature displayed in Figure 2, namely, L-Glu(γ-*p*-methoxyanilide), L-Glu(γ-anilide), and L-Glu(γ-*p*-nitroanilide). Under these conditions, all exchangeable protons would be replaced by deuterons, including those installed on the putative active site general acid. To correct for any possible isotope effect in the detection method, standard curves were determined for each respective aniline in D_2O (extinction coefficient values shown in parentheses in Table 1S).

The kinetic isotope effects thus determined were 1.45 for L-Glu(γ-*p*-methoxyanilide), 1.03 for L-Glu(γ-anilide) and 1.83 for L-Glu(γ-*p*-nitroanilide), suggesting that there is a proton in flight at the rate-limiting transition state of the reaction of each substrate. By way of comparison, similar values (kie = 2−3) have also been obtained (*44*, *47*) for the acylation of chymotrypsin by *p*-OMe and *p*-NO_2 anilides. Our observation of isotope effects with both *p*-OMe and *p*-NO_2 anilides effectively excludes the possibility that the observed curvature of Figure 2 is due to a substituent-dependent change in mechanism where the rate-limiting step for acylation by substrates bearing electron-withdrawing substituents involves rate-limiting C−N bond cleavage prior to rapid protonation of the anionic leaving group. Rather, the isotope effect data and Hammett plot data are consistent with the concerted mechanism proposed in Scheme 3, featuring general-acid-catalyzed breakdown of an initially formed tetrahedral intermediate. Although the observed isotope effect values are smaller than what is usually expected for a rate-limiting general-acid-assisted proton transfer (*48*), they do not rule out our preferred mechanism. Analysis of isotope effects is complex (*48*−*51*), and small values have previously been explained by invoking solvation effects, asymmetric transition states, or nonlinear N−H-X geometries, of which the last two may be particularly pertinent in our case.

pH−*Rate Studies.* To determine the pK_a of the active-site general acid proposed above, experiments were designed to measure the transpeptidation reaction rate at various pH levels. The stability of the purified GGT over the pH range studied was previously confirmed through incubation of the enzyme in buffer at a given pH, followed by verification of the residual enzyme activity of an aliquot of the incubation solution (see Methods). Between the pH values of 7.0 and 9.5, the kinetic parameters of k_{cat} and K_M were measured by the usual method. The observed k_{cat} values for transpeptidation from L-Glu(γ-*p*-nitroanilide) were found to vary by a factor of 5, according to a bell-shaped profile (not shown). Nonlinear regression of the observed k_{cat} values according to eq 2 (see Methods) yielded the kinetic pK_a values of 7.8 and 8.8, indicating that the catalytic mechanism involves one active site amino acid residue that is catalytically competent in its basic form (pK_a ∼ 7.8) and another that is active in its acidic form (pK_a ∼ 8.8). The form and fit of these three profiles are consequently consistent with the ionization, at low pH, of an active site nucleophile (or a general base required to deprotonate such a nucleophile) and the titration, at high pH, of an active site general acid.

Our kinetic pK_a of 7.8 is similar to the kinetic pK_a of 7.0 reported previously for GGT-mediated acyl transfer reaction between L-γ-glutamyl-*p*-nitroanilide and glycylglycine (*52*). For the GGT-mediated hydrolysis of the same anilide substrate, pK_a values of 6.0 (*53*) and 6.1 (*11*) have been reported. This pK_a was initially attributed to a histidine imidazole, and subsequent mutagenesis studies showed that replacement of the two conserved histidine residues of the small subunit of human GGT dramatically reduced (to 2% residual activity) the efficiency of the mutant enzyme. This allows for the involvement of these histidines in a general-acid/base mechanism but does not exclude the possibility that other ionizable groups may be involved (*11*, *53*).

In similar pH−rate profile experiments, the reaction of rat kidney GGT at 37 °C with γ-glutamyl-4-methyl-7-aminocoumarin in the presence of a high concentration of Gly−Gly as an acceptor substrate was studied (*54*). This reaction also displayed a narrow bell-shaped pH-V_{max} profile centered around pH 8.1. In that study, the pH dependence of the acid limb was said to reflect the pK_a of Gly−Gly, the acceptor substrate common to both studies, suggesting that the deprotonated form of Gly−Gly (pK_a = 8.13) is the true acceptor. Our results cannot exclude this possibility, which requires a change of rate-determining step at low pH from the acylation to the deacylation step. The pH dependence of the basic limb of the observed bell-shaped profile was attributed to the ionization of a kinetically critical acidic residue (*54*). Our pH−rate profile results confirm their observations and allow the assignment of a pK_a value of 8.8 to the active site general acid.

The high pK_a of the general acid, relative to that of the theoretical zwitterionic tetrahedral intermediate that would be formed during a sequential acylation mechanism (Scheme 2, pathway 1), suggests that the formation of this intermediate (that is protonation of the anionic tetrahedral intermediate) would be thermodynamically disfavored. The decreased stability of this intermediate would lead to a mechanism featuring a concerted transition state as shown in Scheme 3.

pK_a−Temperature Studies. In an attempt to further characterize the putative general acid of GGT that is responsible for catalysis of the rate-limiting breakdown of the tetrahedral intermediate, the variation of the acidity constant measured from the pH-k_{cat} profile determined for L-Glu(γ-*p*-nitroanilide) at temperatures between 15 and 50 °C was studied. The van't Hoff plot (*55*) of the observed basic kinetic pK_a value versus the reciprocal of the temperature allowed the enthalpy of ionization (ΔH_a) to be determined from the slope. In general, it has been shown that for a carboxylic acid, $\Delta H_a \approx 0$ kcal/mol, whereas for thiols and ammonium ions, $\Delta H_a \approx 7$ kcal/mol (*55*). For the reaction of GGT with L-Glu(γ-*p*-nitroanilide), the enthalpy of the kinetically relevant ionization (basic limb) was found to be 4 ± 2 kcal/mol, consistent with the latter category of acids. Mutagenesis studies (*56*) have shown that the only Cys residue in the light subunit of rat kidney GGT may be replaced by Ala without any appreciable loss of activity, such that the Cys thiol is unlikely to be the putative general acid. Rather, the results of these temperature studies are consistent with the assignment of the general acid as a His imidazolium ion or possibly a primary ammonium ion, which is in turn consistent with the measured pK_a value of 8.8.

Temperature−Rate Studies. Using rate data obtained as a function of temperature varied between 15 and 40 °C at pH 8.0, the enthalpy and entropy of activation for the reaction of GGT with L-Glu(γ-*p*-nitroanilide), L-Glu(γ-anilide) and L-Glu(γ-*p*-methoxyanilide) were determined by constructing Eyring plots of $\ln((k_{cat}h)/(k_BT))$ vs $1/T$ (where h is Planck's constant, k_B is Boltzmann's constant, and T is temperature) (*40*). From these plots, $\Delta H^{\ddagger}$ was calculated from the linear slopes, and $\Delta S^{\ddagger}$ was calculated from the y-axis intercepts for the three acyl donor substrates studied. The values thus obtained were $\Delta H^{\ddagger} = 7.3 \pm 0.3$ kcal/mol and $\Delta S^{\ddagger} = -21.1 \pm 0.9$ cal mol^{-1} K^{-1} for L-Glu(γ-*p*-nitroanilide), $\Delta H^{\ddagger} = 8.3 \pm 0.9$ kcal/mol and $\Delta S^{\ddagger} = -19.0 \pm 2.9$ cal mol^{-1} K^{-1} for L-Glu(γ-anilide), and $\Delta H^{\ddagger} = 8.8 \pm 1.6$ kcal/mol and $\Delta S^{\ddagger} = -16.4 \pm 5.4$ cal mol^{-1} K^{-1} for L-Glu(γ-*p*-methoxyanilide). It is apparent that all three substrates show similar $\Delta H^{\ddagger}$ and $\Delta S^{\ddagger}$ values within experimental error for their acylation reaction with GGT. This suggests that all three acylation reactions pass through transition states that loosely resemble each other (i.e. a common mechanism), but the imprecision of the temperature studies prevents further speculation of their subtle differences. However, it is interesting to compare these results with those obtained for the rate-limiting acylation of chymotrypsin, a serine protease, by neutral amide substrates. For example, the acylation of chymotrypsin by benzoyl-L-tyrosylglycinamide shows a $\Delta H^{\ddagger}$ of 11.5 kcal/mol and a $\Delta S^{\ddagger}$ of −19.8 cal mol^{-1} K^{-1} (*55*), which are very similar to the values obtained herein. This comparison shows that the values obtained for GGT are reasonable for rate-limiting acylation of a serine hydrolase by an amide; however, these data taken alone do not allow us to conclude exclusively that the active site nucleophile of GGT is a hydroxyl group.

On the other hand, the effectiveness of certain hydroxyl-specific inhibitors (such as phenylmethanesulfonyl fluoride (*57*), acivicin (*58*, *59*), DON (*11*), and borates (*11*)) and the apparent oxidative stability of the purified enzyme suggest that the active site nucleophile is more likely to be a hydroxyl group than a cysteine sulfhydryl group. Recent labeling experiments (*60*) with *Escherichia coli* GGT have identified the small subunit *N*-terminal threonine residue (Thr-391) as the active site nucleophile. This threonine residue is conserved among all GGT enzymes whose sequences are known and corresponds to Thr-381 in the human enzyme and Thr-380 in the rat kidney enzyme (*61*). The kinetic data presented herein obtained for rat kidney GGT are consistent with Thr-380 acting as the active site nucleophile and a nearby His imidazolium or primary ammonium group acting as a general acid catalyst of the decomposition of the tetrahedral intermediate leading to acylation. However, other possibilities are equally valid, and more definitive labeling experiments are underway.

In summary, our results provide the first kinetic evidence for the involvement of an active site general acid in the rate-limiting acylation of GGT by γ-glutamyl anilides. Furthermore, this acylation reaction can apparently be accelerated by either electron-withdrawing or electron-donating substituents, suggesting that GGT uses either two mechanisms to catalyze acylation or one concerted mechanism involving kinetic general acid catalysis of aniline departure. The latter interpretation is consistent with the data obtained from the isotope effect, pH−rate, and temperature studies presented herein. The physicochemical values measured in this work for the active site nucleophile or general base (pK_a ~7.8) and general acid (pK_a ~8.8, $\Delta H_a = 4 \pm 2$ kcal/mol) should also assist in the eventual identification of the amino acid residues directly involved in the catalytic mechanism.

ACKNOWLEDGMENT

The authors wish to acknowledge Dr. Christine Desrosiers and the members of her research group at Notre Dame Hospital, Montréal, and Dr. Steven Rowland of Merck-Frosst, Pointe-Claire Dorval, for their generous assistance providing the rat kidneys.

SUPPORTING INFORMATION AVAILABLE

Details of the synthesis of anilides **2a**−**h** and the colorimetric kinetic assay, as well as tables containing the steady-state reaction rates for the various reactions of GGT with L-glutamyl-γ-anilides described herein, are available on request. This material is available free of charge via the Internet at http://pubs.acs.org.

REFERENCES

1. Meister, A. (1973) *Science 180*, 33−39.
2. Meister, A. (1974) *Ann. Intern. Med. 81*, 247−253.
3. Lieberman, M. W., Barrios, R., Carter, B. Z., Habib, G. H., Lebovitz, R. M., Rajagopalan, S., Sepulveda, A. R., Shi, Z. Z., and Wan, D.-F. (1995) *Am. J. Pathol. 147*, 1175−1185.
4. Griffith, O. W., Bridges, R. J., and Meister, A. (1979) *Proc. Natl. Acad. Sci. U.S.A. 76*, 6319−6322.
5. Tate, S. S., and Meister, A. (1974) *J. Biol. Chem. 249*, 7593−7602.

6. Thompson, G. A., and Meister, A. (1975) *Proc. Natl. Acad. Sci. U.S.A. 72*, 1985−1988.
7. Thompson, G. A., and Meister, A. (1977) *J. Biol. Chem. 252*, 6792−6798.
8. Meister, A., Tate, S. S., and Griffith, O. W. (1981) *Methods Enzymol. 77*, 237−253.
9. Tate, S. S., and Meister, A. (1985) *Methods Enzymol. 113*, 400−419.
10. Allison, R. D., and Meister, A. (1980) *J. Biol. Chem. 256*, 2988−2992.
11. Allison, R. D. (1985) *Methods Enzymol. 113*, 419−437.
12. Taniguchi, N., and Ikeda, Y. (1998) *Adv. Enzymol. Relat. Areas Mol. Biol*. 239−278.
13. Thompson, G. A., and Meister, A. (1976) *Biochem. Biophys. Res. Comm. 71*, 32−36.
14. McIntyre, T. M., and Curthoys, N. P. (1979) *J. Biol. Chem. 254*, 6499−6504.
15. Gololobov, M. Y., and Bateman, R. C., Jr. (1994) *Biochem. J. 304*, 869−876.
16. Tate, S. S., and Meister, A. (1981) *Mol. Cell. Biochem. 39*, 357−368-
17. Bradford, M. M. (1976) *Anal. Biochem. 72*, 248−254.
18. Malathi, P., Preiser, P., Fairclough, P., Mallett, P., and Crane, R. K. (1979) *Biochim. Biophys. Acta 554*, 259−263.
19. Goldbarg, J. A., Pineda, E. P., Smith, E. E., Friedman, O. M., and Rutenburg, A. M. (1963) *Gastroenterology 44*, 127−133.
20. Pentz, L., and Thornton, E. R. (1967) *J. Am. Chem. Soc. 89*, 6931−6938.
21. Ménard, A., and Keillor, J. W. (1999) M. Sc. Thesis, Université de Montréal, Montréal, Canada.
22. Jencks, W. P. (1971) *Cold Sp. Har. Sym. Quantum Biol. 36*, 1−11.
23. Jencks, W. P. (1969) *Catalysis in Chemistry and Enzymology*, pp 523−525, McGraw-Hill, New York.
24. Lowry, T. H., and Richardson, K. S. (1987) in *Mechanism and Theory in Organic Chemistry* (Bartlett, A. C., and McCombs, L. W., Eds.), pp 143−159, Harper and Row, New York.
25. Walsh, C. (1979) *Enzymatic Reaction Mechanisms*, pp 667−864, W. H. Freeman and Company, San Francisco, CA.
26. Kluger, R. (1992) in *Mechanisms of Catalysis* (Sigman, D. S., Ed.), pp 271−313, Academic Press, San Diego, CA.
27. Huang, X., Day, N., Luo, X., Roupioz, Y., Seid, M., and Keillor, J. W. (1999) *J. Pept. Res. 53*, 126−133.
28. Swain, C. G., and Langsdorf, W. P. (1951) *J. Am. Chem. Soc. 73*, 2813−2819 and references therein.
29. Swansburg, S., Buncel, E., and Lemieux, R. P. **(**2000) *J. Am. Chem. Soc. 122*, 6594−6600.
30. Jencks, D. A., and Jencks, W. P. **(**1977) *J. Am. Chem. Soc. 99*, 7948−7960.
31. Funderburk, L. H., Aldwin, L., and Jencks, W. P. (1978) *J. Am. Chem. Soc. 100*, 5444−5459.
32. Jencks, W. P. (1972) *Chem. Rev. 72*, 705−718.
33. Fox, J. P., Page, M. I., Satterthwait, A., and Jencks, W. P. (1972) *J. Am. Chem. Soc. 94*, 4729−4731.
34. Jencks, W. P. (1972) *J. Am. Chem. Soc. 94*, 4731−4732.
35. Morgan, M. R. J. (1972) *Enzymologia 42*, 129−137.
36. Osumi, A., Rahmo, A., King, S. W., Przystas, T. J., and Fife, T. H. (1994) *Biochemistry 33*, 14750−14757.
37. Caplow, M., and Jencks, W. P. (1962) *Biochemistry 1*, 883−893.
38. Hall, A. D., and Williams, A. (1986) *Biochemistry 25*, 4784−4790.
39. Matta, M. S., Greene, C. M., Stein, R. L., and Henderson, P. A. (1976) *J. Biol. Chem. 251*, 1006−1008.
40. Bender, M. L., and Nakamura, K. (1962) *J. Am. Chem. Soc. 84*, 2577−2582.
41. Lowe, G., and Yuthavong, Y. (1971) *Biochem. J. 124*, 117−122.
42. Somorin, O., and Ameghashitsi, L. (1987) *Biochem. Intl. 15*, 1189−1196.
43. Petkov, D., Christova, E., Pojarlieff, I., and Stambolieva, N. (1975) *Eur. J. Biochem. 51*, 25−32.
44. Inagami, T., Patchornik, A., and York, S. S. **(**1969) *J. Biochem. 65*, 809−819.
45. Lucas, E. C., and Caplow, M. (1972) *J. Am. Chem. Soc. 94*, 960−963.
46. Sager, W. F., and Parks, P. C. (1963) *J. Am. Chem. Soc. 85*, 2678−2679.
47. Bundy, H. F., and Moore, C. L. (1966) *Biochemistry 5*, 808−811.
48. Jencks, W. P. (1969) in *Catalysis in Chemistry and Enzymology*, pp 243−281, McGraw-Hill, New York.
49. Melander, L.; Saunders, W. H., Jr. (1980) *Reaction Rates of Isotopic Molecules*, pp 202−224, Wiley-Interscience, New York.
50. Schowen, R. L. (1972) *Prog. Phys. Org. Chem. 9*, 275−332.
51. More-O'Ferrall, R. A. (1975) in *Proton-Transfer Reactions* (Calden, E. F., and Gold, V., Eds.), p 201, Wiley, New York.
52. PetitClerc, C., Schiele, F., Bagrel, D., Mahassen, A., and Siest, G. (1980) *Clin. Chem. 26*, 1688−1693.
53. Ikeda, Y., Funjii, J., and Taniguchi, N. (1996) *J. Biochem. 119*, 1166−1170.
54. Cook, N. D., and Peters, T. J. (1985) *Biochim. Biophys. Acta 832*, 142−147.
55. Tipton, K. F., and Dixon, H. B. F. (1979) *Methods Enzymol. 63*, 183−234.
56. Ikeda, Y., Funjii, J., Taniguchi, N., and Meister, A. (1995) *J. Biol. Chem. 270*, 12471−12475.
57. Inoue, M., Horiuchi, S., and Morino, Y. (1978) *Biochem. Biophys. Res. Comm. 82*, 1183−1188.
58. Stole, E., Smith, T. K., Manning, J. M., and Meister, A. (1994) *J. Biol. Chem. 269*, 21435−21439.
59. Smith, T. K., Ikeda, Y., Funjii, J., Taniguchi, N., and Meister, A. (1995) *Proc. Natl. Acad. Sci. U.S.A. 92*, 2360−2364.
60. Inoue, M., Hiratake, J., Suzuki, H., Kumagai, H., and Sakata, K. (2000) *Biochemistry 39*, 7764−7771.
61. Sakamuro, D., Yamazoe, M., Matsuda, Y., Kangawa, K., Taniguchi, N., Matsuo, H., Yoshikawa, H., and Ogasawara, N. (1988) *Gene 73*, 1−9.

BI011234D